Ionic motion in bioactive ceramics investigated by dielectric spectroscopy

Peter Lunkenheimer, H. Rall, J. Alkemper, H. Fuess, R. Böhmer, Alois Loidl

Angaben zur Veröffentlichung / Publication details:

Lunkenheimer, Peter, H. Rall, J. Alkemper, H. Fuess, R. Böhmer, and Alois Loidl. 1995. "Ionic motion in bioactive ceramics investigated by dielectric spectroscopy." *Solid State Ionics* 81 (1-2): 129–34. https://doi.org/10.1016/0167-2738(95)00170-b.

Ionic motion in bioactive ceramics investigated by dielectric spectroscopy

P. Lunkenheimer [a], H. Rall [a], J. Alkemper [b], H. Fuess [b], R. Böhmer [c], A. Loidl [a]

[a] *Institut für Festkörperphysik, Technische Hochschule Darmstadt, 64289 Darmstadt, Germany*
[b] *Fachbereich Materialwissenschaft, Technische Hochschule Darmstadt, 64287 Darmstadt, Germany*
[c] *Institut für Physikalische Chemie, Johannes Gutenberg Universität, 55099 Mainz, Germany*

Abstract

Measurements of the complex ionic conductivity of a bioactive glass ceramic and related materials are reported for frequencies 0.1 Hz $\leq \nu \leq$ 500 MHz and at temperatures 10 K $\leq T \leq$ 600 K. Depending on frequency and temperature, the data show blocking-electrode effects, low frequency dispersion, hopping conduction and relaxation processes. The relevance of our results for the surgical application of this material is discussed.

1. Introduction

Recent advances in the preparation of glass ceramics have led to the development of numerous applications of these materials. One example is the use of phosphate-based glass ceramics as hard tissue replacement [1]. These ceramics are bioactive, i.e. a linkage of natural and artificial bone is achieved by exchange of ions. Therefore it is of vital importance to obtain knowledge about the nature of the ionic transport processes in these materials. For that purpose measurements of the complex ac conductivity in a broad frequency and temperature range are an ideal tool. In this article we present the results of measurements of the ac conductivity of a bioactive phosphate glass ceramic in a temperature range of 10 K $\leq T \leq$ 600 K and a frequency range of 0.1 Hz $\leq \nu \leq$ 500 MHz. In addition, time domain measurements have been performed. For comparison, the dielectric response of the glassy starting material, of two related glass ceramics of similar composition and of a commercially available bioactive material has been investigated.

2. Experimental

Glasses of composition P_2O_5–Al_2O_3–CaO–Na_2O–F^- (with mass fractions of 0.504 : 0.101 : 0.155 : 0.172 : 0.01) were prepared by melting at 1100°C and quenching. Devitrification is achieved by a subsequent heat treatment at temperatures well above 500°C. To obtain homogeneous bulk crystallization, a nucleation agent (FeO, 5.7 wt%) was added. Apart from $AlPO_4$, apatite [$Ca_5(PO_4)_3X$, X = F, OH] and an iron containing orthophosphate with $NaZr_2(PO_4)_3$ structure (NASICON-type), X-ray diffraction, electron microscopy and nuclear magnetic resonance have revealed the appearance of

three structurally unknown pyrophosphates [2]. Several specimens were obtained from the glassy ingot: Sample A, crystallized at 700°C, contains all phases mentioned above. A glass ceramic with fluoro apatite as main crystalline phase can be obtained if the glass is kept at 520°C for 6 hours (sample B). For comparison, a glass ceramic with ZrO_2 as nucleation agent was prepared (sample C). It contains $NaZr_2(PO_4)_3$ as the primary crystalline phase. In addition, we investigated the glassy starting material (sample D) and the commercially available bony tissue replacement material Endobon® (sample E, Merck, Darmstadt) which is fabricated from cattle bones and exhibits a highly porous macroscopic structure.

Platelets of typical dimensions $5 \times 10 \times 0.5$ mm^3 were covered by silver paint or gold electrodes on opposite sides to form electrical contacts. For the preparation of sample E the original Endobon® sample was pulverized and afterwards pressed to pellets of dimensions similar to those of the other samples.

Measurements of the complex conductivity $\sigma = \sigma' + i\sigma''$ were carried out in broad frequency and temperature ranges using different experimental setups. For frequencies 0.1 Hz $\leq \nu \leq$ 100 Hz a frequency response analyser supplemented with a high impedance preamplifier has been used (Schlumberger 1260 and Chelsea dielectric interface). The frequency range 20 Hz $\leq \nu \leq$ 1 MHz was covered using the autobalance bridge HP4284. The high frequency data ($\nu \geq 1$ MHz) were recorded using an HP4191 impedance analyser connected to the cooling/heating device via an air line [3]. In addition, time domain measurements were obtained by recording the time dependent current after the application of a constant voltage on the sample.

Most of the measurements were performed in a nitrogen gas heating system covering a temperature range 10 K $\leq T \leq$ 600 K. In addition, a closed cycle refrigerator and various ovens have been used.

3. Results and discussion

Fig. 1 shows the temperature dependence of the real part of the conductivity σ' of the glass ceramic A for various frequencies. Obviously, different processes contribute to the conductivity and give rise to a rather complicated behaviour:

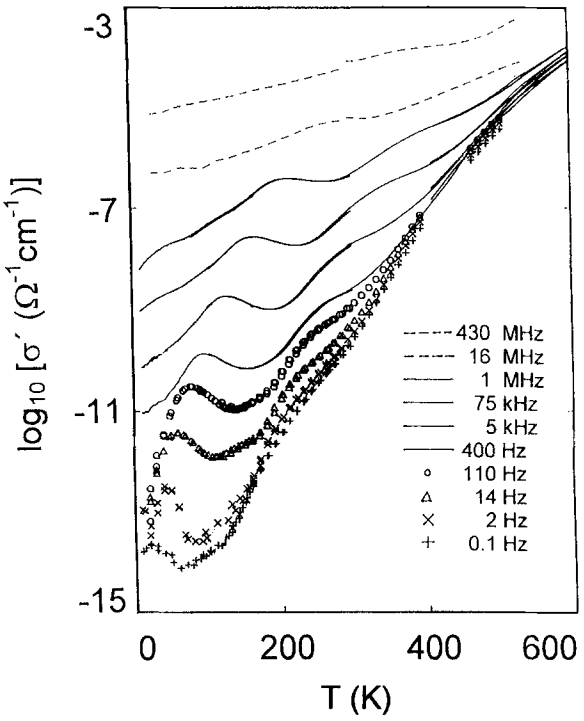

Fig. 1. Temperature dependence of the real part of the conductivity σ' of sample A for various frequencies.

(i) At high temperatures and low frequencies all $\sigma'(T)$ curves approach the one obtained at 0.1 Hz which therefore could be interpreted as dc limit, at least above approximately 350 K. For $T > 350$ K, $\sigma'(T)$ can be fitted by an Arrhenius law, $\sigma' = \sigma_0/(k_B T) \exp(-E_{dc}/k_B T)$. This finding implies the existence of a thermally activated process in sample A. An energy barrier of 0.76 eV can be deduced.

(ii) The deviations from the Arrhenius law at low temperatures and/or high frequencies are predominantly due to ac conductivity.

(iii) In addition to these global transport processes there are at least two local relaxation processes which most probably stem from hops of ions in local double well potentials.

Detailed information on the ac conductivity can be obtained from Fig. 2 where we have plotted the frequency dependence of σ' for various temperatures in a double logarithmic representation. At high frequencies and low temperatures the overall behaviour is governed by a power law, $\sigma' \sim \nu^s$, with $s \approx 0.7$ which is typical for hopping conductivity [4].

Superimposed on this power law are two peaks which can be identified with those seen in Fig. 1. At low frequencies and high temperatures $\sigma'(\nu)$ exhibits a very weak frequency dependence, $\sigma' \sim \nu^{\alpha}$, $\alpha = 0.07$. In this range the real and the imaginary parts of the dielectric constant ϵ decrease with the same power law as is demonstrated for 505 K in the inset of Fig. 2. Such a behaviour, called low frequency dispersion (LFD), is often explained in terms of electrochemical processes [5]. For LFD the ratio ϵ''/ϵ' is expected to be related to the exponent α via $\epsilon'/\epsilon'' = \tan(\alpha\pi/2)$. The resulting $\alpha = 0.08$ compares favourably with the value of 0.07 as deduced from $\sigma'(\nu)$.

At the highest temperatures and towards low frequencies the slope of $\sigma'(\nu \to 0)$ increases again which indicates the onset of blocking electrode effects, which is a characteristic feature of ionic conductors. The blocking of the electrodes has been characterized by time domain measurements performed at 600 K. Fig. 3 shows the time dependence of the current I subsequent to the application of a constant voltage to the sample (solid line). Two power laws $I \sim t^{-m}$ can be identified with exponents $m \approx 0.1$ for $t < 100$ s and $m' \approx 0.25$ for $t > 100$ s. After approximately 8×10^4 s the polarity of the voltage has been reversed. Now the time dependence shows a similar behavior (dashed line) but the crossover between the two power laws occurs at a much later time of $t \approx 10^3$ s. The Fourier transformation of a power law $I \sim t^{-m}$ leads to a frequency dependence $\sigma' \sim \nu^{m}$ [5]. Therefore the change of slope in Fig. 3 can be identified with the transition from LFD to blocking electrode behaviour. After the change of polarity the ions have to cross almost the entire sample before they reach the opposite electrode leading to a much later occurrence of blocking electrode effects, as observed experimentally. From the crossover time and the sample thickness the drift velocity of the ions can be estimated as $v \approx 4 \times 10^{-7}$ m/s. From the current density j, the density of charge carriers can be deduced via $j = nev$ as $n \approx 10^{18}$ cm^{-3}. Even if this calculation is oversimplified, it clearly shows, that only a small fraction of Na^+ and Ca^{2+} ions (ppm level) are mobile.

In order to gain closer insight into the dynamics of the two relaxation processes seen in Fig. 1, in Fig. 4 we have plotted the frequency of the peak maxi-

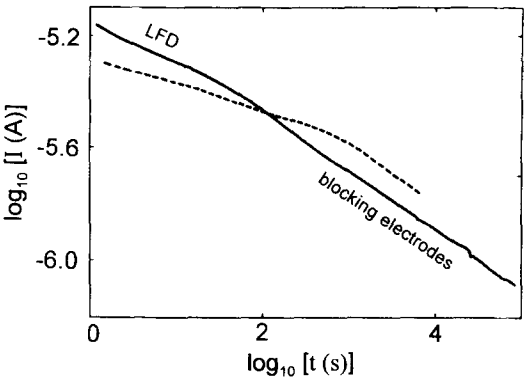

Fig. 3. Time dependent current after application of a constant voltage. The solid line has been obtained after the first application of the dc voltage. The dashed line shows the time dependence after a change of polarity.

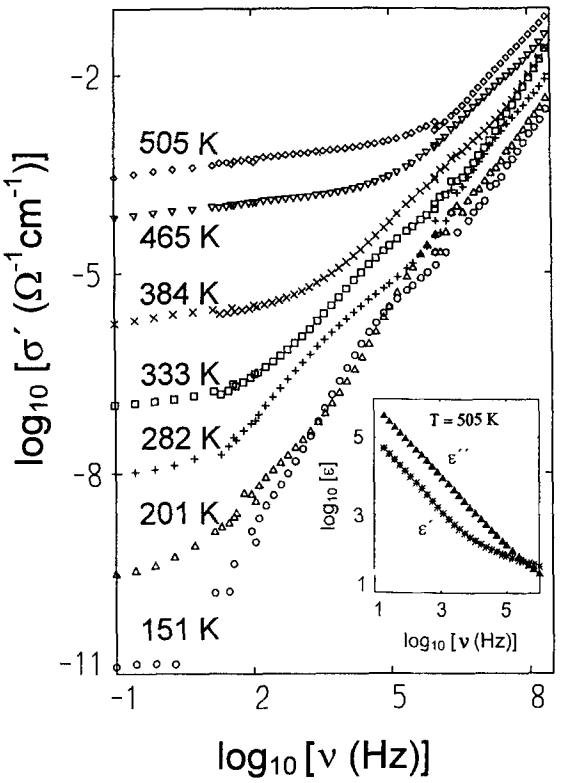

Fig. 2. Frequency dependence of the real part of the conductivity σ' of sample A for various temperatures. The inset shows the frequency dependence of the complex dielectric constant for $T = 505$ K.

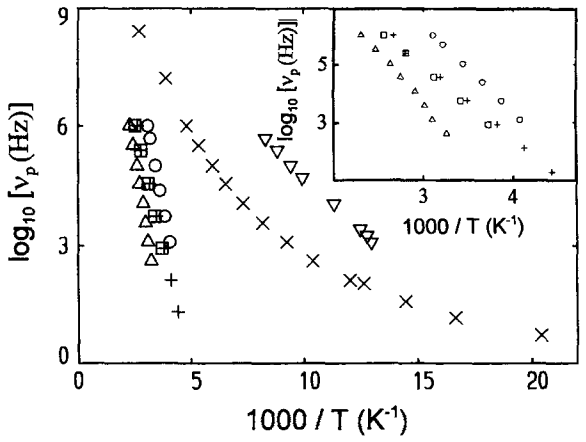

Fig. 4. Logarithm of the frequency of the relaxation peak maximum versus inverse temperature for samples A (×, +); B (○); C (□) and E (△, ▽).

mum (determined after subtraction of the conductivity background) versus temperature in an Arrhenius representation. The high temperature peak (+) exhibits thermally activated behaviour, $\nu_p = \nu_0 \exp(-E_1/k_B T)$ with $E_1 = 0.52$ eV and $\nu_0 = 10^{13}$ Hz. The temperature dependence of the low temperature relaxation (×) can be described by an Arrhenius type of behaviour for temperatures $T > 150$ K with parameters $E_2 = 0.21$ eV and $\nu_0 = 10^{11}$ Hz. However, there are clear deviations from the Arrhenius law at lower temperatures. At the lowest temperatures accessible, the data are compatible with an effective energy barrier of 0.02 eV, although it cannot be ruled out that the peak frequencies become temperature independent for $T < 5$ K.

It appears natural to assume that the different relaxation processes in the complex bioactive material are due to the different (crystalline) phases from which it is made up. To find out which local environments within the glass ceramic give rise to each of the two relaxation peaks, we have performed comparative measurements in the precursor glass, sample D, and in the glass ceramics, B and C, which contain fluoro apatite or $NaZr_2(PO_4)_3$ (NASICON-structure) as the primary crystalline phases, respectively. We find, that the glass (sample D) shows no signs of electrical relaxation processes, however both ceramic samples exhibit one relaxation process each. The peaks found in glass ceramic B follow an Arrhenius behaviour with $E = 0.6$ eV and $\nu_0 = 10^{15}$ Hz (Fig. 4 (○)). The temperature dependence of the relaxation peak found in sample C (□) shows very good agreement with that of the high temperature process in sample A (inset in Fig. 4). Therefore in glass ceramic A this process can be attributed to the crystallites with NASICON-structure. In addition, Fig. 4 contains results on sample E (Endobon®) which exhibits two relaxation processes with $E = 0.23$ eV and $E = 0.73$ eV for the low and high temperature relaxation, respectively.

A peak associated with the low temperature relaxation in sample A has been found neither in sample B nor in sample C. However, there are indications that the low temperature process may be associated with the elementary hopping process responsible for the dc conductivity seen at high temperatures. This conjecture can be checked directly using theoretical predictions concerning the relation of the energy barrier E_{loc} of the local relaxation process and that of the global dc conduction process (E_{dc}) in ionic conductors [6]. Assuming that the relaxation rate is constant for the single ion jumps but slows down according to t^{-s} as soon as cooperativity sets in, it can be shown that $E_{loc} = (1 - s)E_{dc}$. Here s is the frequency exponent characterizing $\sigma(\nu)$. Recently, the validity of this relation has been demonstrated in a Li-conducting aluminosilicate glass ceramic [7]. With $s = 0.7$, $E_{loc} = 0.21$ eV, and $E_{dc} = 0.76$ eV this relation is also obeyed in our sample. Therefore both, conductivity and low temperature relaxation, most probably arise from the same crystalline phase of the sample.

The deviation from Arrhenius behaviour of the low temperature process can be ascribed either to quantum mechanical tunneling or to two different energy barriers for high and low temperatures. However, the latter explanation seems unlikely as this would imply a very low attempt frequency for the low temperature process of 10^4 Hz (or lower) as can be deduced from Fig. 4. A tunneling process seems most likely in the hydroxy apatite structure shown in Fig. 5, that is exhibited by parts of the glass ceramic. Here the observed relaxation process could arise from a hopping of the proton of the OH^- ion between two positions on either side of the oxygen which may be accompanied by a shift of the O^- ion along the c axis. The proton has a high tunneling probability due to its low mass [8]. It is noted that in

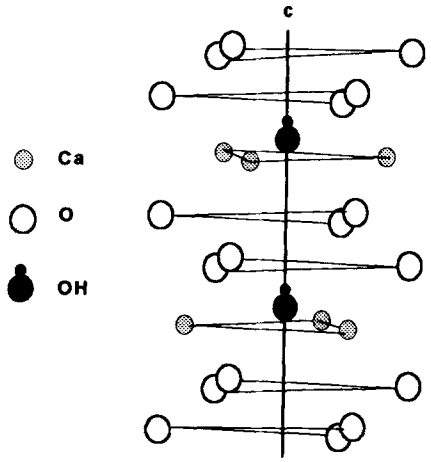

Fig. 5. Schematic coordination of OH^- groups in hydroxy-apatite

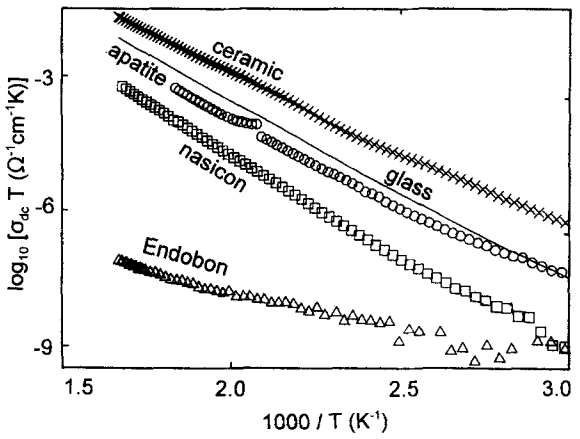

Fig. 6. Arrhenius plot of the conductivity at 20 Hz for samples A (×); B (○); C (□); D (line) and E (△).

sample B which contains fluoro-apatite as main crystalline phase a low temperature relaxation process was not detected.

Fig. 6 shows the temperature dependence of the conductivity at 20 Hz for all samples investigated in an Arrhenius representation. The energy barriers and conductivity prefactors deduced from Fig. 6 are given in Table 1. As demonstrated in Fig. 6, sample A clearly exhibits the highest conductivity which most probably is the reason for its high level of bioactivity. Remarkably, the Endobon® sample E has the lowest conductivity of all samples investigated. We found similar values for different samples of Endobon®, which have been subjected to different grinding procedures and pressures during preparation. From this we can exclude grain boundary effects as reason for the low conductivity of sample E. The low conductivity of Endobon® is mainly due to the low value of its prefactor σ_0, which can be written as $\sigma_0 = na^2q^2\ \nu_0/(k_BT)$ if one assumes a simple periodic potential energy [9]. Here n is the density of charge carriers of charge q, a is the distance between two potential wells and ν_0 is the attempt frequency. It seems unreasonable that the hopping distance or the attempt frequency of Endobon® are some orders of magnitude smaller than that of the other materials investigated. Therefore, most probably, the small conductivity prefactor in Endobon® is due to a low density of charge carriers. At the temperature of the human body, σ_{dc} of Endobon® is about three orders of magnitude lower than that of the glass ceramic. This leads to the conclusion that the good suitability of Endobon® as bone substitute material is not due to its ionic conductivity but is mainly caused by its high porosity. Guided by these results it would be worthwhile to test if the bioactivity of Endobon® can be increased by adding small ions like Na^+ or Ca^{2+} as dopants and if the bioactivity of the artificial ceramic can be increased by increasing the porosity of the material.

4. Summary

The complex ac conductivity of a bioactive alkali-phosphate glass ceramic has been measured in a broad frequency and temperature range. At high frequencies and low temperatures hopping conduc-

Table 1
Energy barrier and prefactor of the dc conductivity as determined from Fig. 6

Sample	A (ceramic)	B (apatite)	C (NASICON)	D (glass)	E (Endobon®)
E_{dc} (eV)	0.76	0.82	0.95	0.85	0.49
σ_0 ($K\Omega^{-1}$ cm^{-1})	60	20	80	120	0.001

tion of ions is the dominant charge transport process. In addition, at low frequencies and high temperatures LFD and blocking electrode effects have been found which gives evidence for ions as dominant charge carriers. In addition, there are two relaxation processes superimposed on the conductivity. The high temperature process has been found to arise from the NASICON structured crystalline component of the sample. Most probably, the low temperature process is associated with motions of OH^- ions in the hydroxy-apatite phase of the ceramic. In order to discuss the relevance of our results in relation to the biochemically important electrolyte transport it is pointed out that the mobile ions most likely are Na^+, Ca^{2+} and OH^-. However, the relatively low level of conductivity of the highly bioactive Endobon® sample indicates the importance not only of the ionic conductivity but also of the macroscopic structure of bone replacement materials. The multitude of relaxational processes in the bioactive glass ceramic points to the existence of different pathways adapted to the various charge carriers. The ion transport across the interface connecting artificial and natural tissue appears to be of particular importance for the understanding and optimising of the surgical application. In order to address these questions, further electrochemical studies would certainly be most helpful.

Acknowledgements

We thank J. Hemberger for helpful discussions. This work has been supported by the Deutsche Forschungsgemeinschaft under Grant No. SFB262-D5. The Endobon® samples have been kindly supplied by Merck, Darmstadt.

References

[1] P. Wange, J. Vogel, L. Horn, L. Höland and W. Vogel, Silicates Indust. 7–8 (1990) 231.
[2] C. Schulz, G. Miehe and H. Fuess, Z. Kristallogr. 209 (1994) 249.
[3] R. Böhmer, M. Maglione, P. Lunkenheimer and A. Loidl, J. Appl. Phys. 65 (1989) 901.
[4] See e.g. S.R. Elliott, Adv. Phys. 36 (1987) 135; A.R. Long, Adv. Phys. 31 (1982) 553.
[5] A.K. Jonscher, J. Mat. Sci. 26 (1991) 1618.
[6] K.L. Ngai, Comm. Solid State Phys. 9 (1979) 127; 9 (1980) 141.
[7] R. Böhmer, G. Gerhard, F. Drexler, A. Loidl, K.L. Ngai and W. Pannhorst, J. Non-Cryst. Solids 155 (1993) 189.
[8] N. Hitmi, C. LaCabanne and R.A. Young, J. Phys. Chem. Solids 47 (1986) 533.
[9] A.B. Lidiard, in: Handbuch der Physik, Band XX, ed. S. Flügge (Springer, Berlin, 1957) pp. 275–279.